INSULATION RESISTANCE AND LEAKAGE CURRENTS IN MLCCs WITH CRACKS

Alexander Teverovsky

Dell Services Federal Government, Inc.
NASA/GSFC Greenbelt, MD20771, USA
Alexander.A.Teverovsky@nasa.gov

INTRODUCTION

Low-voltage multi-layer ceramic capacitors, MLCC, constitute the majority of electronic components used in most applications. Failures of these parts are often related to cracks that are caused either by insufficient process control during manufacturing, thermal shock associated with soldering, or flex cracking during handling and/or mechanical testing of the circuit boards. Analysis of the effectiveness of test methods allegedly ensuring MLCC quality is important for the part selection process in high-reliability applications.

It is generally assumed that Insulation Resistance (IR) depends on the capacitance value and is the same for different case sizes and rated voltages (VR). At +25 °C, military specifications require IR to be greater than 100,000 MΩ or 1,000 MΩ-μF, whichever is less, and at +125 °C, 10,000 MΩ or 100 MΩ-μF, whichever is less. Variations of IR by an order of magnitude as temperature varies from room to 125 °C corresponds to activation energy of ~0.3 eV, which is much lower than the values reported for conductivity of ceramic materials.

High volumetric efficiency commercial MLCCs have somewhat relaxed requirements. For example, Murata requires a minimum IR of 500 MΩ-μF for capacitors greater than 0.047 μF.

The limiting values of IR for both, military and commercial MLCCs are inversely proportional to the value of capacitance, *C*, and do not depend on VR and the size (thickness of the dielectric) of capacitors. This implies that the specific resistivity of ceramics used in MLCCs, ρ, is constant: $IR = (\rho\times\varepsilon\times\varepsilon_0)/C$, where ε is the dielectric constant. However, this contradicts to experimental data that indicate that leakage currents, hence ρ, changes substantially with the electric field [1].

The value of IR is determined as the ratio of VR to the current measured within 1 or 2 minutes of electrification. However, mass production of MLCCs requires high-speed testing techniques. Hence, manufacturers are looking for test systems that will allow IR measurements in much shorter periods of time, within seconds of electrification [2].

Currents in MLCCs decrease with time relatively slowly after the application of a voltage step. This behavior is due to the dielectric relaxation processes that might include dipole orientation, redistribution of ionic charges, charge injection from electrodes, or electron tunneling into the traps in the dielectric [1]. Disregarding the specific physical mechanism of relaxation, a process of decreasing currents with time can be described as charge absorption. Absorption currents can be defined as polarization (under applied voltage) and depolarization (under short circuit condition) currents.

Absorption processes occur in all dielectric materials employed in the different types of capacitors, including MLCCs [3-5]. Absorption currents typically follow the empirical Curie - von Schweidler law, referred to as a Kohlrausch behavior in some publications [6]. According to this law, polarization currents decrease with time as a power function,

$$I(t) = I_0 \times t^{-n}, \qquad (1)$$

where I_0 and n are constants, and n is close to 1.

Intrinsic leakage currents, I_{il}, in MLCCs are attributed to electron injection from metal electrodes [5]. However, there is no agreement in literature on the mechanism of electron transport. The mechanism of conduction through ferroelectric materials was attributed to the electrode-limited Schottky emission [7-9], bulk-limited Poole-Frenkel transport [10-11], or space charge limited conduction, SCLC [12-13].

Two screening procedures that are used during the manufacturing of MLCCs are often considered sensitive to the presence of defects in the dielectric: measurements of the dielectric withstanding voltage (DWV) and measurements of the insulation resistance (IR). Our previous work [14] analyzed the effectiveness of DWV screening to reveal capacitors with cracks, and this study is focused on the effectiveness of IR measurements.

In the assessment of the effectiveness of IR measurements, it is important to understand (i) which currents are measured during the standard testing, (ii) the relationship between the leakage currents caused by cracking and the absorption and intrinsic leakage currents at normal conditions (room temperature and rated voltage), and (iii) the dependence of currents on temperature and voltage. The purpose of this work is to gain insight into absorption and leakage currents in low-voltage MLCCs, investigate voltage and temperature dependencies of these currents, and assess the sensitivity of IR measurements to the presence of cracks.

EXPERIMENT

A variety of low-voltage (rated to 100 V or less) MLCCs produced by seven different vendors was used in this study to reveal common characteristics in absorption and leakage currents. Most of the parts were commercial, high volumetric efficiency, X7R capacitors with EIA case sizes from 0402 to 2225, voltage ratings from 6.3 V to 100 V, and capacitances from 1500 pF to 100 μF.

Mechanical defects in MLCCs were introduced using three techniques:

- Mechanical fracture. A corner portion of the part was chipped-off using fine cutters.
- Surface cracking. A capacitor was damaged by impact on the surface with a Vickers indenter.
- Thermal shock. Capacitors were stressed either by a cold thermal shock using the ice water testing (IWT) technique or hot thermal shock using a solder dip test [15].

These techniques were used to simulate manufacturing or assembly/handling related cracking in ceramic capacitors and have different advantages and drawbacks in approaching this goal. Mechanical fracturing guarantees that the internal electrodes are exposed to the environmental conditions, but the charge transport processes on the cleaved surface might be somewhat different in comparison to the processes in cracks. IWT produces cracks that are initially filled with water, which proves difficult to remove completely, even after baking at high temperatures. Cracks caused by solder dip testing might be tiny and difficult to detect. The indenter causes localized damage most closely simulating real-life cracking, however, there is no guarantee that the cracks penetrate deep enough to cross the internal electrodes. In all cases described in this work, optical examination and/or additional testing in humid environments verified the presence of cracks that extended through the active area of the capacitors.

ABSORPTION AND LEAKAGE CURRENTS IN MLCCS

Typical absorption currents in ceramic capacitors after the application of rated voltages are shown in Fig. 1. In double logarithmic coordinates, *I-t* characteristics can be approximated with straight lines over a long period of time, typically from seconds to several hours. This confirms the applicability of the power law, Eq. (1). The absorption currents were reproducible, thus measurements on group sizes of up to 20 samples showed that all parts had close amplitudes and rates of decay. The currents increased with capacitance and depending on the part type, the exponent *n* varied in the range from 0.6 to 1.1. For Mfr. C, 1 μF, 6.3 V capacitors (Fig. 1.a), the currents leveled off after ~ 1 hour due to the absorption currents decreasing below the intrinsic leakage currents. Comparing the polarization and depolarization absorption currents (Fig. 1.b), showed that in all cases, the currents were similar. Analysis of current relaxation in ceramic capacitors with different types of dielectric materials (X7R, X5R, and NPO/COG) confirmed Curie - von Schweidler behavior in all cases.

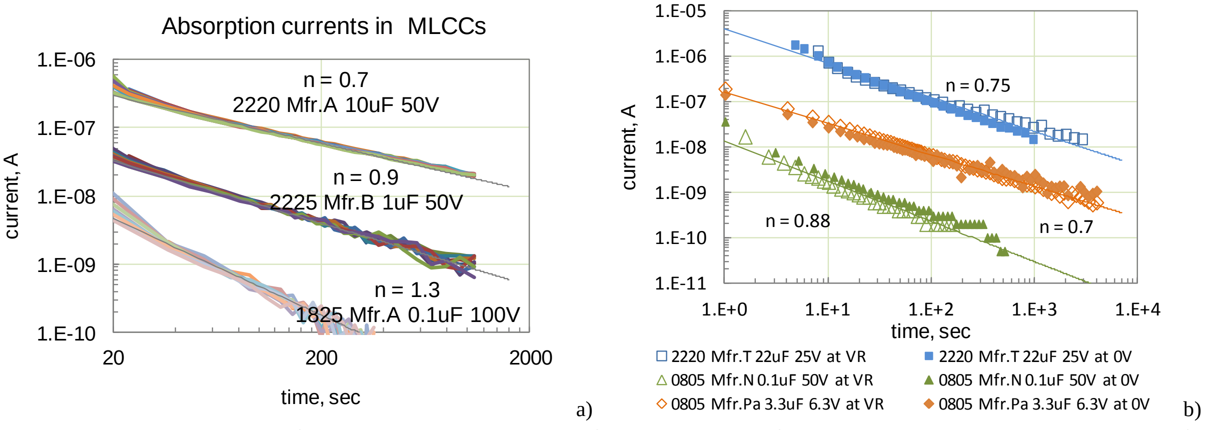

Fig. 1. Time dependence of currents in X7R MLCCs after application of rated voltages. (a) Reproducibility of absorption(polarization) currents measured for 5 to 10 samples in three types of capacitors. (b) Comparison of polarization (empty marks) and depolarization currents (solid marks) in three types of MLCCs from different vendors.

Effect of Size

The distribution of currents measured in three groups of 1 μF, 50 V capacitors in different case sizes (EIA codes 2220, 1210, and 0805) are shown in Fig. 2.

These parts were produced by the same manufacturer using the same materials, but had different dielectric thicknesses: 19.4 μm for 2220, 8.9 μm for 1206, and 4.3 μm for 0805 capacitors. The currents were measured after 60 seconds and 1000 seconds of polarization. No substantial difference was observed for the 60-sec measurements; however, the 1000-sec measurements were almost an order of magnitude less for the 2220 parts, compared to the 0805 capacitors. The results can be explained by considering that currents measured after 1000 seconds have a substantial component related to the intrinsic leakage currents, whereas the absorption currents prevailed during the 60-sec measurements. The intrinsic leakage currents have a strong dependence on the electric field, and subsequently, on the thickness of the dielectric. In contrary, the absorption currents depend mostly on the value of capacitance.

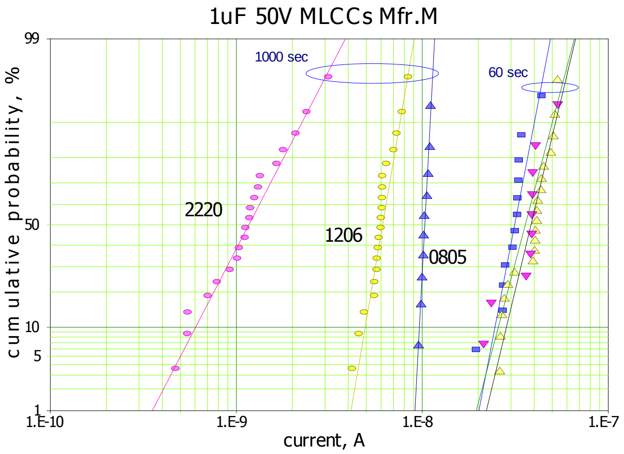

Fig. 2. Distribution of leakage currents in 1 μF, 50V capacitors measured after 60 seconds and 1000 seconds of electrification. All parts were from the same manufacturer, but had different case sizes. The thickness of the dielectric was 19.4 μm, 8.9 μm, and 4.3 μm for EIA case sizes 2220, 1206, and 0805, respectively.

Effect of Capacitance

Correlation between the values of IR measured by a standard technique and capacitance for 40 different part types is shown in Fig. 3. The best fit approximation indicates that IR is inversely proportional to the capacitance: IR = 5×10^9/C, where C is in μF and IR is in Ω. This relationship is similar to the one used by manufacturers of low-voltage, high-value MLCCs to set the limiting value of the resistance: IR = 5×10^8/C. Experimental data are approximately 10 times greater than the specified value, which gives a reasonable value for the manufacturing margin.

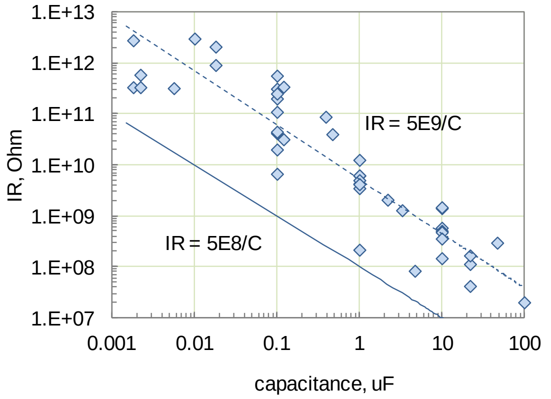

Fig. 3. Variations of IR with capacitance for different types of MLCCs rated to voltages from 6.3 V to 100 V. Solid line corresponds to the specification data for IR limits for commercial parts.

Effect of Voltage

Typical I-t characteristics for 10 μF, 16 V capacitors, measured at different voltages, are shown in Fig. 4. An increase in the applied voltage leads to an increase in the absorption currents, whereas the rate of current decay, characterized by the exponent n, remains practically the same. At voltages approximately twice the rated voltage, the current decay levels-off after 1000 seconds, due to increased I_{il}.

Absorption currents that were measured after 120 seconds of polarization for four types of MLCCs are plotted against voltage in Fig. 5 and indicate a linear dependence of I_{120} on voltage. The slopes of the lines represent the variation in IR values from 2.4×10^{8} Ω to 1.5×10^{10} Ω, for different part types. These IR values display no voltage dependence up to at least twice the rated voltage.

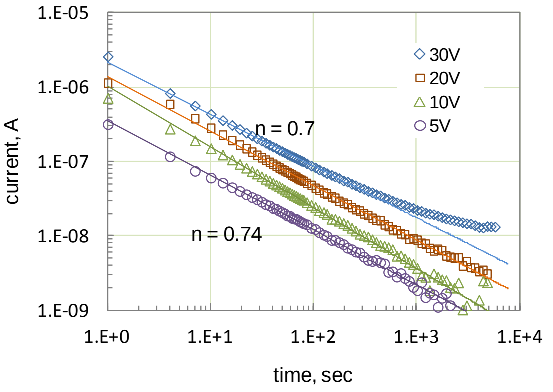

Fig. 4. Relaxation of currents in case size 1206, 10 μF, 16 V, capacitors at voltages from 5 V to 30 V.

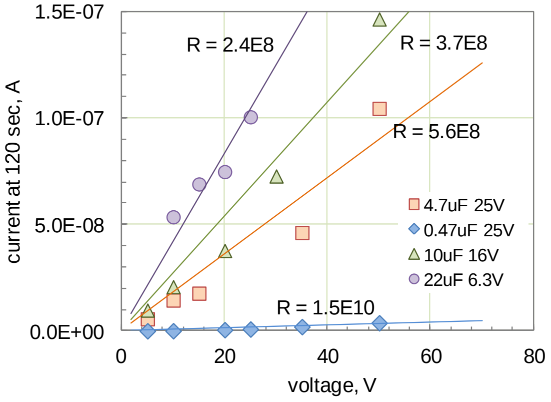

Fig. 5. Voltage dependence of currents measured after 120 seconds of polarization in four different types of case size 1206, X7R capacitors (see legends).

Variations of polarization and depolarization currents with voltage for 3.3 μF, 6.3 V and 22 μF 6.3V capacitors are shown in Fig. 6. The absorption (depolarization) currents increase linearly to ~ 20 V, and then saturate with voltage. At voltages exceeding ~ 3VR, intrinsic leakage currents after ~ 100 sec of polarization became greater than absorption currents and the measured current does not change significantly with time.

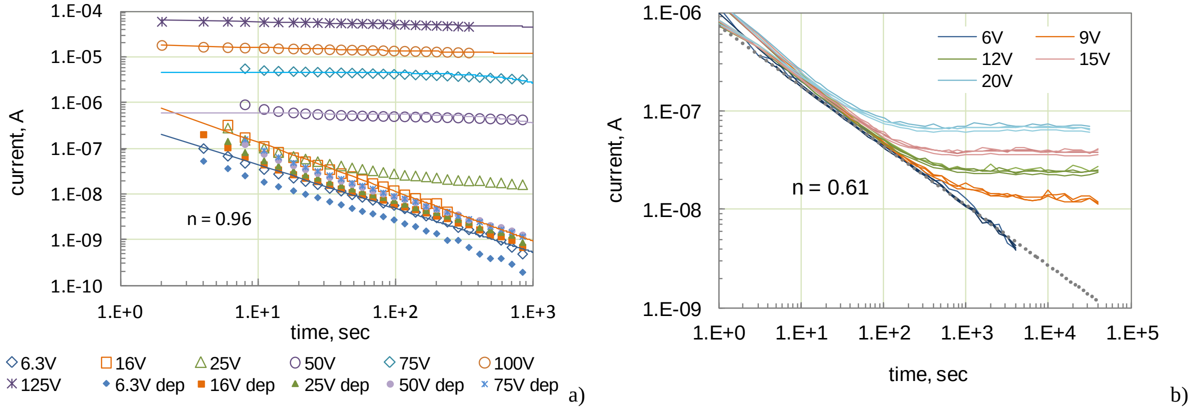

Fig. 6. Time dependence of absorption currents at different voltages. (a) Polarization (empty marks) and depolarization (solid marks) currents for case size 0805, 3.3 μF, 6.3 V capacitors. (b) Polarization currents for 22 μF 6.3V capacitors in case 1206.

Examples of *I-V* characteristics for different types of MLCCs that were measured based on the intrinsic leakage currents are shown in Fig. 7. At room temperature, experimental data can be approximated with straight lines in Schottky, *ln(I)* vs. $V^{0.5}$, coordinates. However, at high temperatures, a better fit is obtained in double logarithmic coordinates, which suggests that the current is a power function of voltage, $I \sim V^{m}$, where *m* is constant. The slope of the room temperature *I-V* curves in Schottky coordinates varied from 0.9 $(\mathrm{m/V})^{0.5}$ to 1.1 $(\mathrm{m/V})^{0.5}$. At high temperatures, the exponent *m* varied within a relatively narrow range, from 1.42 to 1.52. Similar results were obtained for different part types manufactured by different vendors. This indicates that at high temperatures, *I-V* characteristics of most X7R capacitors follow the 3/2 power law.

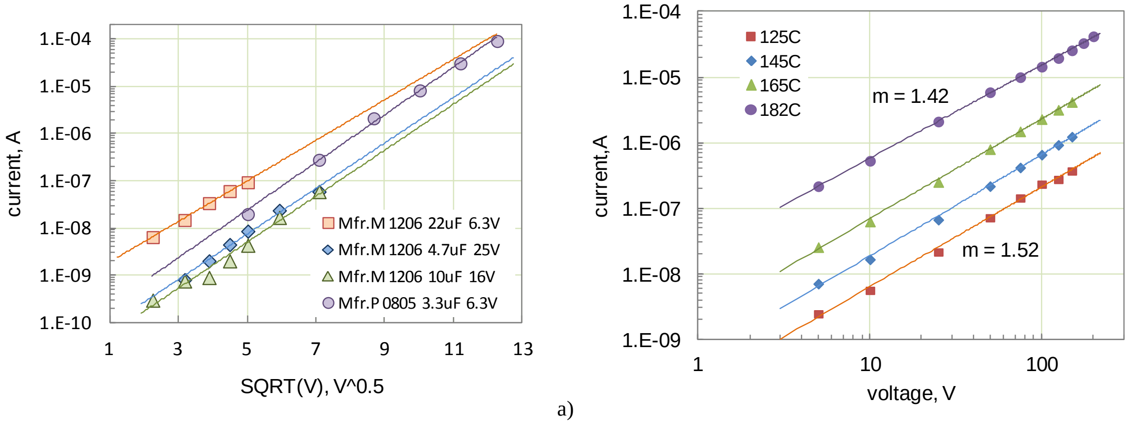

a) b)

Fig. 7. *I-V* characteristics of X7R capacitors. (a) Room temperature characteristics in Schottky coordinates for different part types. (b) High temperature characteristics for case size 2225, 1 µF, 50 V capacitors.

Effect of Temperature

The relaxation of currents measured at rated voltages and temperatures varying from room (300 K) to cryogenic (200 K and 36 K) showed that *I-t* characteristics did not change substantially (see example in Fig. 8.a). Depolarization currents in capacitors at room temperature were close to those measured at temperatures up to 165°C (see an example in Fig. 8.b). Similar results were obtained for different types of X7R capacitors from different vendors, which suggest that absorption currents have weak temperature dependence.

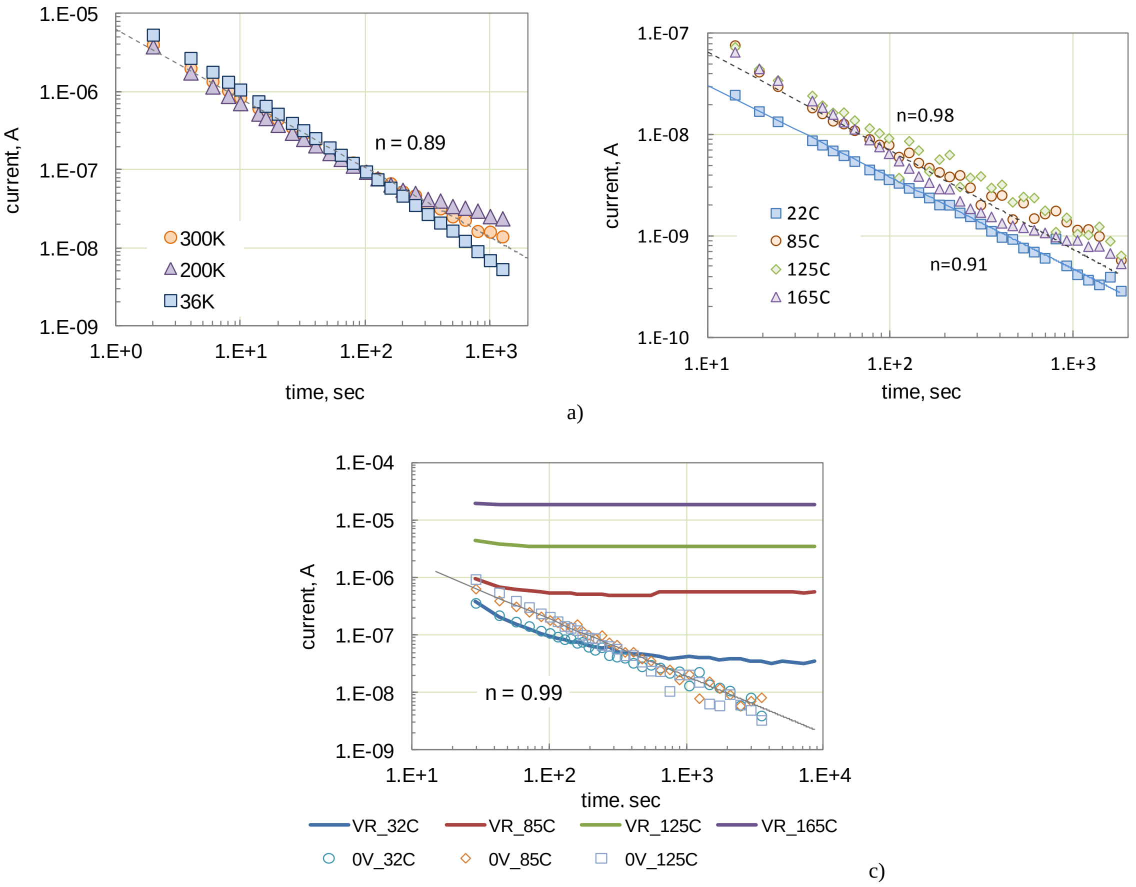

a) b)

c)

Fig. 8. Effect of temperature on current relaxation. (a) Case size 2220, 100 µF, 6.3 V, capacitors at room (300K) and cryogenic (200 K and 36 K) temperatures. (b) Case size 1825, 0.47 µF, 50V, capacitors at temperatures from 22°C to 165°C. (c) Case size 1206 22 µF 6.3V capacitors, lines – polarization, and marks are depolarization currents.

Contrary to that, intrinsic leakage currents increased with temperature exponentially. Examples of temperature dependencies of I_{il} at different voltages are shown in Fig. 9. In Arrhenius coordinates, straight lines accurately approximate the experimental data with the slopes that indicate the activation energy, E_a. In all cases, the slope decreased with the voltage, indicating a decrease in the activation energy. Typically, E_a decreases by 10% to 30% as the voltage increases from 0.5 V/VR to 5 V/VR. At rated voltages, the activation energy for different part types varies from 0.6 eV to 1.3 eV.

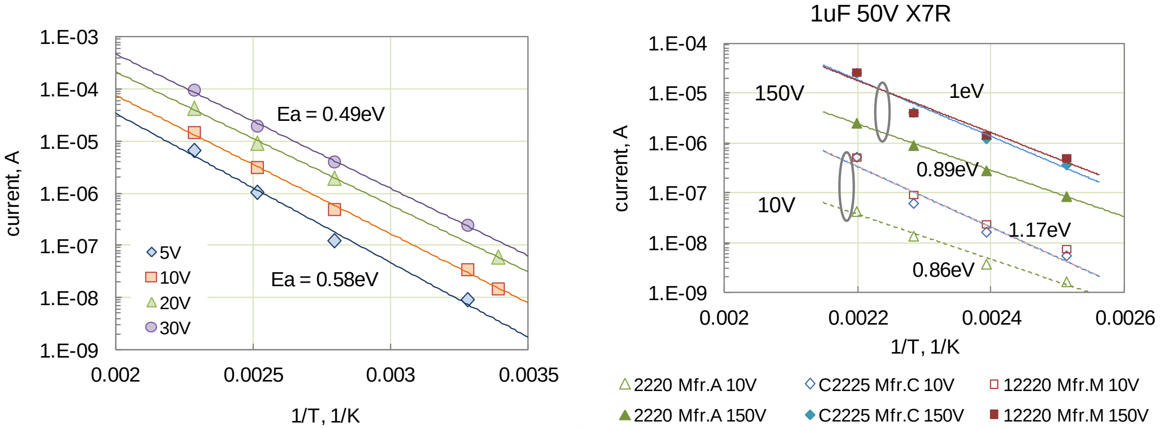

a) b)

Fig. 9. Temperature dependence of leakage currents in Arrhenius coordinates. (a) Case size 1206, 22 μF, 6.3V, capacitors at different voltages. (b) 1 μF, 50 V capacitors from different manufacturers.

Effect of Dielectric Cracking

Current relaxation was measured at different voltages and temperatures for a variety of normal quality (virgin) ceramic capacitors and for a variety of cracked capacitors. In all cases, except for a few involving severely damaged capacitors, absorption currents (both, polarization and depolarization) were similar for virgin and damaged parts. Examples of these measurements at room temperature are shown in Fig. 10.

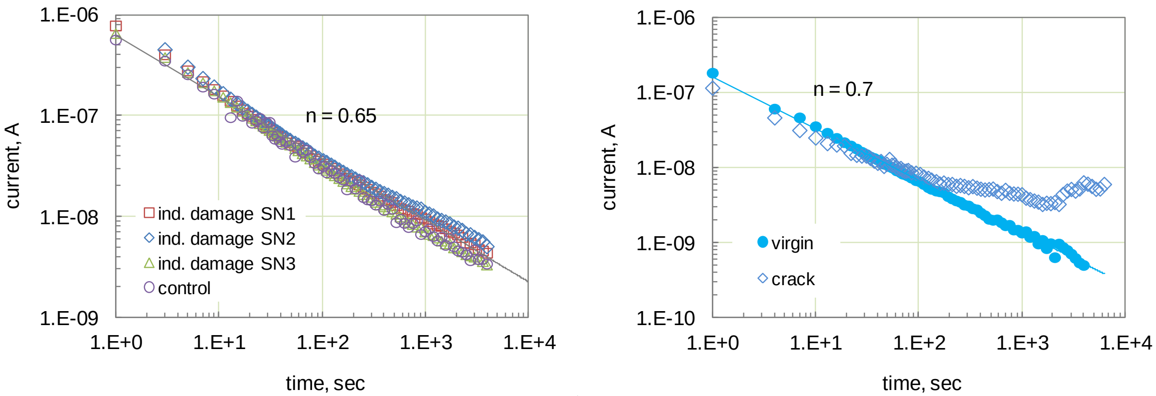

a) b)

Fig. 10. Relaxation of currents in normal and fractured capacitors at room temperature and rated voltages. (a) Case size 1812, 1 μF, 50 V capacitors. (b) Case size 0805, 3.3 μF, 6.3 V capacitors.

For EIA1812, 1 μF, 50 V capacitors, no difference was observed between the normal quality parts and cracked parts within a one-hour period of polarization (Fig.10.a). Fig. 10.b presents an example of a situation when leakage currents in a capacitor with cracks exceeded currents in a normal part. However, this difference was observed only after ~ 100 seconds of polarization, making it undetectable by regular IR measurements.

Correlation between IR values measured after 120 seconds of electrification for 15 different types of virgin and fractured capacitors at room temperature is shown in Fig. 11.a. The data are closely correlated, indicating that IR screening at room temperature would not detect fractured capacitors.

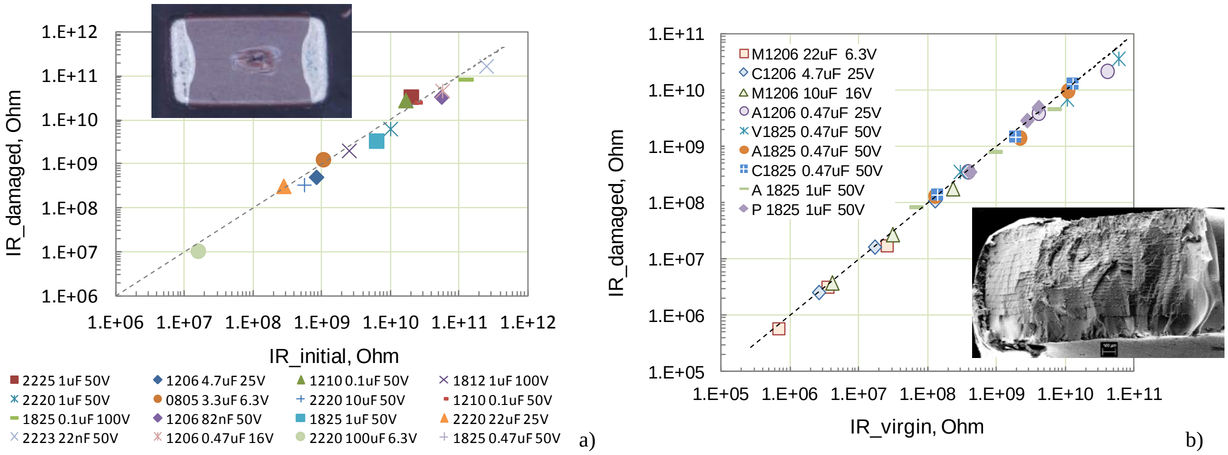

Fig. 11. Effect of cracking on insulation resistance in different types of ceramic capacitors. The IR measurements were carried out using a standard technique: 120 seconds of electrification at rated voltages. The dashed line corresponds to no-change values. (a) Room temperature measurements. (b) Measurements at 85°C, 125°C, and 165°C. Inserts show examples of fractured capacitors used for IR measurements.

It is often assumed that IR measurements at high temperatures (typically 125 °C) are more sensitive to the presence of defects, and thus are more effective in evaluating the quality of capacitors. To assess the effectiveness of high-temperature measurements, nine types of virgin and fractured capacitors were measured at 85°C, 125°C, and 165°C. Results of these measurements are shown in Fig. 11.b. High temperature IR measurements were also closely correlated, indicating that the temperature increase does not assist in revealing mechanical defects in MLCCs. Obviously, this is due to a high level of intrinsic leakage currents that substantially exceed the currents associated with the presence of cracks.

ABSORPTION CAPACITANCE

If a charge, Q_t, that is transferred into the dielectric during polarization, or is released during depolarization, increases with voltage linearly, the absorption process can be described by a capacitance, C_t, that is determined as $C_t = Q_t/V$. The value of Q_t was calculated by approximating the absorption currents with a power law, Eq.(1) and integrating with time over a period from 1 sec. to 10^4 sec.

Variations of Q_t with voltage for 4 types of capacitors are shown in Fig. 12. Below 2VR the charge increases with voltage linearly, and the slopes of the lines allow for estimations of C_t. For the capacitors shown in Fig. 12, the values of C_t were comparable to the nominal values of capacitance and varied from 0.6 µF, for 2.2 µF capacitors, to 39 µF, for 100 µF capacitors. Additional experiments showed that Q_t varies linearly at relatively low voltages, and saturates at voltages exceeding 3VR.

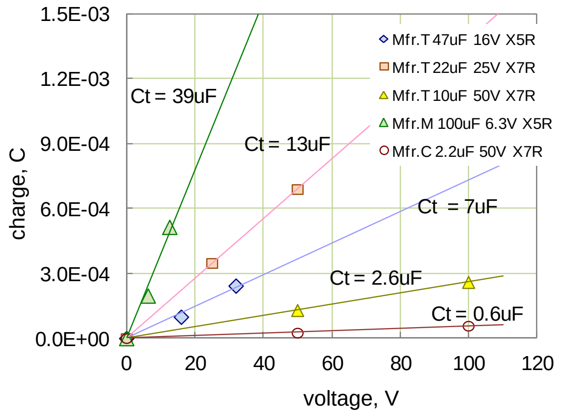

Fig. 12. Variations of absorption charges in different types of EIA2220, X7R/X5R MLCCs. The absorption capacitance (C_t) was calculated as the slope of the $Q_t – V$ lines.

Absorption capacitance was found to be greater for larger valued capacitors, and a correlation between the standard capacitance value at 1 kHz, C_0, and absorption capacitance, C_t was determined (see Fig. 13). For most capacitors, C_t was in the range from 10% to 50% of the nominal value. On average, $C_t = 0.25×C_0$.

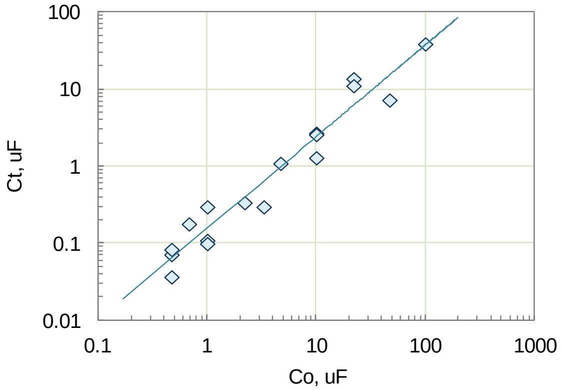

Fig. 13. Correlation between the absorption and nominal values of capacitance for 17 different types of X7R MLCCs.

MODELING OF ABSORPTION CURRENTS

An equivalent circuit of a capacitor that accounts for the effects related to dielectric absorption was suggested first for polystyrene capacitors by Dow in 1958 [16] and is presented in Fig. 14. The capacitor has a nominal value, C_0. Resistor R_{il} is due to the intrinsic leakage currents, and R_d is related to mechanical defects.

Dow have showed that most absorption polarization processes in capacitors can be described by a circuit with five r-C_t relaxators connected in parallel to C_0 by a proper selection of the relaxation times, $\tau_i = r_i \times C_{ti}$, and absorption capacitances, C_{ti}. If a step voltage, V_0, is applied at $t = 0$, variations of the current with time can be given by a simple equation:

$$I(t) = \frac{V_0}{R_d} + \frac{V_0}{R_{i\,l}} + \sum_i \frac{V_0}{r_i} \exp\left(-t/\tau_i\right) \qquad (2)$$

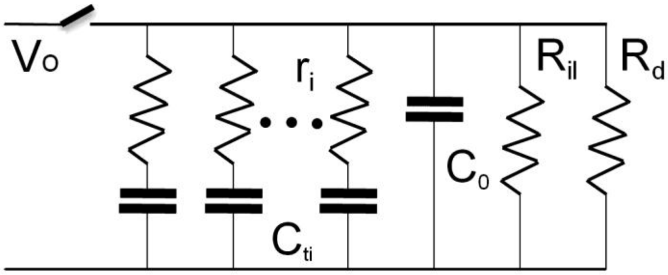

Fig. 14. Dow model of a capacitor with absorption.

Analysis shows that the exponent n in the Curie - von Schweidler law, Eq. (1), is equal to 1 if C_{ti} is constant and r_i increases exponentially for each consecutive relaxator. Experimental data for capacitors with a relatively slow decay, $n < 1$, can be simulated by increasing C_{ti} for larger r_i, and for parts with $n > 1$, by decreasing C_{ti} for larger r_i.

An example of calculations of absorption currents for a 4.7 µF capacitor using four relaxators is shown in Fig. 15. When the absorption capacitance increases in relaxators with larger resistances, as it is shown in Fig. 15.a, then the slope of I-t curve decreases. For instance, if $C_{ti} = i \times 1$ µF, and the values of r_i increase from $10^8\ \Omega$ for $C_{t1} = 1$ µF to $10^{11}\ \Omega$ for $C_{t4} = 4$ µF, the exponent $n = 0.83$. By decreasing absorption capacitances in relaxators with larger resistances, the rate of current decay can be increased, e.g. for $C_{ti} = 0.33 \times C_{ti-1}$, $n = 2$ (see Fig. 15.b).

Obviously, by adding more R-C relaxators with characteristic times below 10^2 sec. or above 10^5 sec. the applicability of the Curie - von Schweidler law can be extended to a more considerable range of times.

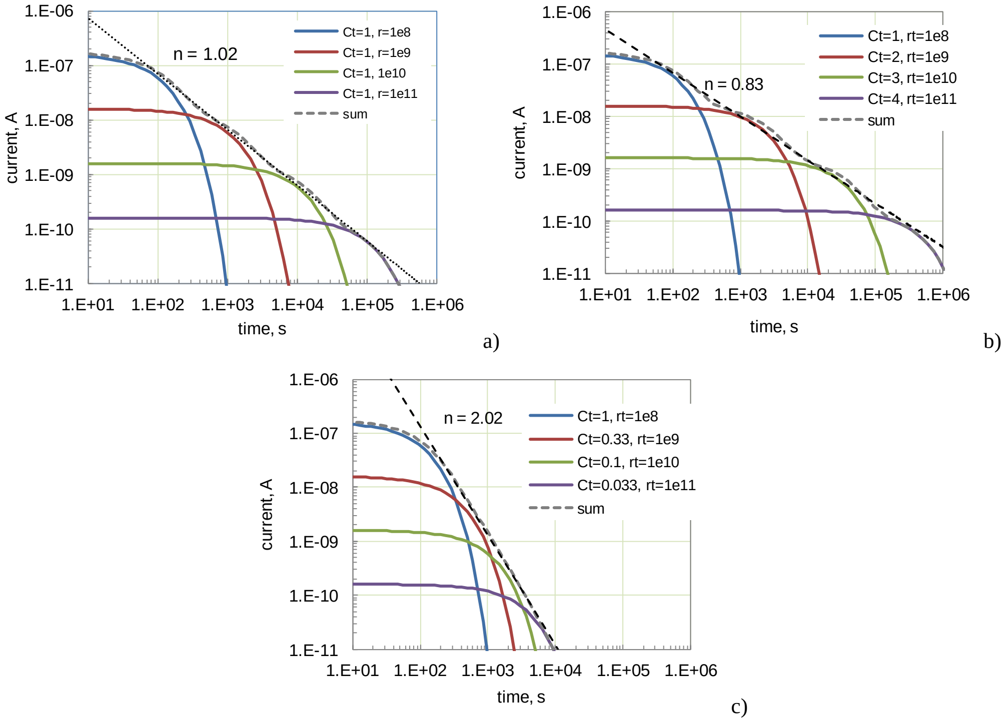

a) b) c)

Fig. 15. Simulation of absorption currents in 4.7 μF capacitors using an equivalent circuit (Fig.14) with four relaxators. (a) C_{ti} is constant. (b) C_{ti} increases for relaxators with larger r_i. (c) C_{ti} decreases with larger r_i.

DISCUSSION

In a general case, the current in a capacitor under step voltage V can be presented as:

$$I(t,T,V) = I_{abs}(t,V) + I_{il}(T,V) + I_{d}(T,V,RH) \qquad (3)$$

This presentation reflects time *(t)*, temperature *(T)*, voltage *(V)*, and relative humidity (RH) dependence of different components of the current. As it has been shown above, absorption currents, $I_{abs}(t,V)$, decrease with time according to a power law (Eq. 1), increase linearly with voltage below 2VR to 3VR, and have a weak dependence on temperature. Intrinsic leakage currents, $I_{il}(T,V)$, do not vary with time, increase exponentially with temperature, and increase super-linearly with voltage. For relatively short testing periods (below 1-hour) and voltages close to VR, possible degradation processes that might affect I_{il}, e.g. migration of oxygen vacancies, are considered negligible. Crack-related leakage currents, $I_d(T, V, RH)$, depend also on the relative humidity of the environment.

For quality assurance purposes, it is important to assess the defect-related component of the current. To optimize test conditions (voltage, temperature and duration), we need to better understand the effect that external factors (T, V, RH) have on the different components in Eq. (3).

Absorption Currents

Our data show that absorption currents dominate during standard IR measurements, and the leakage currents at room temperature might be revealed only after hours of polarization. At relatively low voltages, typically below 2-3 times VR, I_{abs} linearly increases with voltage and does not depend on temperature. Depolarization (short circuit) currents flow in the opposite direction, but have the same isochronic values as polarization currents. These findings are consistent with literature data [1, 13] and can be explained assuming that the absorption process is due to the tunneling of electrons from electrodes into states (traps) located in the forbidden energy gap of the dielectric at the interface with the metal electrodes. Different states have different probabilities of trapping, which results in substantial (exponential) variations of the characteristic times of the process. For the traps uniformly distributed over the energy gap, the characteristic times would change by orders of magnitude, which is consistent with the Dow model. Different distributions of the trap density with energy explain variations of the exponent in the Curie - von Schweidler law.

A close location of the traps to electrodes (likely within dozens of angstroms) results in most of the trapped charges flowing back to the electrodes under shorting conditions, and hence in the reversibility of the absorption process. Charges that are trapped within the bulk of the dielectric would be emptied towards both electrodes, resulting in a negligible current in the external circuit. A saturation of absorption currents at high voltages, which was observed in several cases, is due to the traps filling-up and can be used to assess their concentration, N_t, based on values of the absorption capacitance C_t. It has been shown that C_t is proportional to the value of the nominal capacitance, $C_t = \alpha\times C_0$, where α is a constant that is close to 0.25 at voltages up to ~ 3VR. In this case:

$$C_t = \frac{q\times N_t\times S}{3\times VR} = \alpha\frac{\varepsilon\times\varepsilon_0\times S}{d} \tag{4}$$

where, d is the thickness of the dielectric, S is the surface area of electrodes, ε is the dielectric constant of ceramic at 1 kHz, $q = 1.6\times10^{-19}$ C is the electron's charge, and $\varepsilon_0 = 8.89\times10^{-14}$ F/cm is the dielectric constant in vacuum. From Eq. (4), the value of N_t can be calculated as:

$$N_t = 3\alpha\frac{\varepsilon\times\varepsilon_0\times VR}{d\times q} \tag{5}$$

Assuming that for a typical X7R capacitor, VR is in the range from 6 V to 50 V, d from 5 µm to 15 µm, and $\varepsilon\approx 3000$, N_t is in the range from 1.8×10^{13} cm^{-2} to 6×10^{13} cm^{-2}.

Relatively large values of C_t (~ 25% of C_0) result in large characteristic times, $\tau_i = r_i\times C_t$, even for relatively small resistances r_i. This allows for absorption currents to remain large for a sufficiently long period of time (~120 sec), affecting IR measurements. Assuming for simplicity that only one relaxator, r–C_t, prevails during the period of IR measurements, Δt ~100 sec, and that $\tau = r\times C_t > \Delta t$, the insulation resistance can be presented as:

$$IR = \left(\frac{1}{R_d}+\frac{1}{R_{il}}+\frac{1}{r}\right)^{-1} \tag{6}$$

If the resistance, r, associated with the electron trapping process is less than the resistance associated with the mechanical defects and intrinsic conduction, then $IR\approx r$.
In this case the requirement $\tau > \Delta t$ can be written in the form:

$$IR = r > \frac{100\times10^6}{0.25\times C_0} = \frac{4\times10^8}{C_0}\ , \tag{7}$$

where, C_0 is in µF and r is in Ω. This corresponds to the manufacturers' requirements for IR = $5\times10^8/C_0$, and explains the results presented in Fig. 3.

Intrinsic Leakage Currents

Contrary to the absorption currents, intrinsic leakage currents increase with voltage super-linearly. At sufficiently high voltages (typically exceeding 2VR), these currents dominate the total current through a capacitor after a few seconds of polarization.

The Schottky equation is applicable to systems that have a mean free path of electrons with a thickness greater than that of the dielectric, which is not valid for MLCCs. It has been shown [17] that for ferroelectric thin films, the corrected form suggested by Simmons [18] provides a better agreement with experimental data. According to Simmons, for insulators having small electronic mean free paths, a modified equation can be written as:

$$J_S = AT^{3/2}\mu E\exp\left(-\frac{\Phi_B}{kT}\right)\exp\left(\frac{\beta_s E^{0.5}}{kT}\right), \tag{8}$$

where, A = 3.08×10^{-4} A/cm^2_K$^{1.5}$, µ is the electron mobility in the insulator, and β_s is the Schottky constant:

$$\beta_s = \left(\frac{q^3}{4\pi\varepsilon\varepsilon_0}\right),$$

where, k is the Boltzmann constant, T is the absolute temperature, and ε ~5.5 is the high-frequency dielectric constant for ferroelectric ceramics.

Analysis of *I-V* characteristics at room temperature showed that experimental values of the slopes are in a reasonable agreement with the Simmons model: the ratio of the experimental and calculated slopes was found being in the range from 0.7 to 1.5.

Approximation of *I-V* characteristics with a power law at high temperatures (from 125°C to 165°C) for different capacitors resulted in close values of the exponent m (≈ 1.5). This type of *I-V* characteristic can be attributed to SCLC in the case of injection from pointed electrodes. Lee et al. [5] and Burton [13] observed the near 3/2 power dependence of currents on voltage for Z5U and X7R capacitors. The results were explained by electron emission from electrode protuberances and asperities, which are considered a dominant cause of leakage currents in MLCCs. The presence of electrode protuberances in their work was confirmed through cross section and scanning electron microscopy (SEM), which indicated the irregular nature of the electrodes.

Our cross-sectional examinations did not reveal substantial irregularities in the electrodes, and considering that the same *I-V* characteristics were observed for parts from different manufacturers, it appears more likely that the 3/2 law is due to some intrinsic irregularities in the distribution of the electric field caused by the micro-grain structure of ceramic materials. However, more analysis is necessary to understand this behavior.

All models predict Arrhenius-like temperature dependence of the intrinsic leakage currents. Experimental values of E_a, calculated at relatively low voltages for different part types, vary from 0.6 eV to 1.3 eV. These values are close to the values reported for X7R capacitors by Lee, Burton, et al. [5, 13], from 1.2 eV to 1.3 eV. A decrease of E_a with applied voltage is in qualitative agreement with the Simmons model, Eq. (8).

Manufacturers' data on temperature dependence of IR, in the range from room temperature to 125°C and the requirements in military specifications, indicate much lower values of the activation energy, from 0.27 eV to 0.32 eV. This is due to the different nature of the currents measured at room temperature and at 125°C. Absorption currents that have weak temperature dependence prevail in the first case, and intrinsic leakage currents with activation energy ~ 1 eV prevail during the high temperature measurements.

Considering that the values of IR measured at high temperatures correspond to the intrinsic leakage currents, extrapolation of IR measured at 125°C to room temperature using experimental data of E_a would result in resistance values exceeding 10^{14} Ω, which is far above the values corresponding to the absorption currents.

Leakage Currents Caused by Cracks

Although the voltage and temperature dependence of the damage-related leakage currents is not known, this dependence is most likely less significant compared to the intrinsic leakage currents. For this reason, attempts to screen-out damaged capacitors by IR measurements at high voltages and/or temperatures are not effective.

Based on the results presented in this work, crack-related leakage currents, in most cases, are below the absorption currents. Some improvement of the sensitivity of IR measurements to the presence of cracks might be achieved by increasing the duration of the electrification period. For example, at $0.6 < n < 1.1$, an increase of Δt from 1 min to 1 hour would reduce I_{abs} by 12 to 90 times and thus increase the possibility of detecting excessive currents in the part. However, in many cases, crack-related leakage currents are small, and development of new techniques for their detection is necessary. One such technique is based on measurements of absorption voltages (to be published). Using this technique it was shown that capacitors with cracks might have very high levels of resistance, from 10^9 Ω to 10^{13} Ω. Note that based on the current IR requirements, these parts would be considered acceptable. This means that both the testing technique and the requirements should be revised.

Preliminary results show that humidity, even at relatively low levels (~ 50% RH), might strongly affect the behavior of parts with dielectric cracks. Monitoring the degradation of leakage currents after exposure to humid environments might be useful in detecting defective capacitors.

CONCLUSION

1. Absorption currents prevail during standard measurements of insulation resistance in MLCCs at room temperature. These currents follow the Curie - von Schweidler power law, with the exponent varying from 0.6 to 1.1. Polarization and depolarization currents are reproducible, have opposite polarity, and their isochronic values are similar. Absorption currents have a weak dependence on temperature, change linearly with voltage up to 2 - 3 times VR, and stabilize at larger voltages.

2. Absorption processes in MLCCs can be explained by electron trapping in states at the metal/ceramic interface, as a result of tunneling. Absorption capacitance increases with the nominal value of capacitance, and is on average ~25% of C_0. The effective concentration of the interface traps is in the range from 1.8×10^{13} cm^{-2} to 6×10^{13} cm^{-2}.

3. At low temperatures, intrinsic leakage currents in MLCCs can be described using the Simmons model. At temperatures above 85°C, *I-V* characteristics follow a power law with the exponent close to 1.5. Activation energy of leakage currents for different types of X7R capacitors is in the range from 0.6 eV to 1.3 eV.

4. Neither room temperature nor high temperature standard IR measurements are sensitive to the presence of cracks.

Development of new, more effective testing methods to reveal capacitors with mechanical defects is necessary.

ACKNOWLEDGMENT

This work was sponsored by the NASA Electronic Parts and Packaging (NEPP) program. The author is thankful to Michael Sampson, NEPP Program Manager, for support of this investigation, Bruce Meinhold, MEI Technologies, Inc., Senior Components Engineering Manager for a review and discussions.

REFERENCES

[1] G. G. Raju, "*Dielectrics in electric fields*": CRC Press, Marcel Dekker, p.^pp. 592, 2003.

[2] R. Anklekar, J. Fish, J. Christofferson, and V. Cooke, "Insulation Resistance Testing of High-Capacitance BME Multilayer Ceramic Capacitors," in *CARTS'03, the 23th Symposium for Passive Components*, Scottsdale AZ, 2003, pp. 86-95.

[3] X. Xu, M. Niskala, A. Gurav, M. Laps, and K. Saarinen, "Advances in Class-I C0G MLCC and SMD Film Capacitors," in *The 28th symposium for passive components, CARTS'07*, Newport Beach, CA, 2008.

[4] H. Bachhofer, H. Reisinger, H. Schroeder, T. Haneder, C. Dehm, H. Von Philipsborn, and R. Waser, "Relaxation effects and steady-state conduction in non-stoichiometric SBT films," *Integrated Ferroelectrics,* vol. 33, pp. 245-252, 2001.

[5] H. Y. Lee, K. C. Lee, J. N. Schunke, and L. C. Burton, "Leakage currents in multilayer ceramic capacitors," *IEEE Transactions on Components Hybrids and Manufacturing Technology,* vol. 7, pp. 443-453, 1984.

[6] H. Kliem, "Kohlrausch relaxations: new aspects about the everlasting story," *Dielectrics and Electrical Insulation, IEEE Transactions on,* vol. 12, pp. 709-718, 2005.

[7] J. H. Koh, B. M. Moon, and A. Grishin, "Dielectric properties and Schottky barriers in silver tantalate-niobate thin film capacitors," *Integrated Ferroelectrics,* vol. 39, pp. 1361-1368, 2001.

[8] L. Pintilie, I. Vrejoiu, D. Hesse, G. LeRhun, and M. Alexe, "Ferroelectric polarization-leakage current relation in high quality epitaxial Pb(Zr, Ti)O-3 films," *Physical Review B,* vol. 75, Mar 2007.

[9] J. C. Shin, J. Park, C. S. Hwang, and H. J. Kim, "Dielectric and electrical properties of sputter grown (Ba,Sr)TiO3 thin films," *JOURNAL OF APPLIED PHYSICS,* vol. 86, pp. 506-513, Jul 1999.

[10] E. Loh, "A model of dc leakage in ceramic capacitors," *Journal of Applied Physics,* vol. 53, pp. 6229-6235, 1982.

[11] P. Zubko, D. J. Jung, and J. F. Scott, "Electrical characterization of PbZr0.4Ti0.6O3 capacitors," *Journal of applied physics,* vol. 100, Dec 2006.

[12] F. D. Morrison, P. Zubko, D. J. Jung, J. F. Scott, P. Baxter, M. M. Saad, R. M. Bowman, and J. M. Gregg, "High-field conduction in barium titanate," *Applied Physics Letters,* vol. 86, Apr 2005.

[13] L. C. Burton, "Intrinsic mechanisms of multilayer ceramic capacitor failure," Virginia Polytechnic Inst. and State Univ., Blacksburg, VA, ADA199113, 1998, pp. 1-57. Available:

[14] A. Teverovsky, "Breakdown Voltages in Ceramic Capacitors with Cracks," *IEEE Transactions on Dielectrics and Electrical Insulation,* vol. 19, pp. 1448-1455, 2012.

[15] A. Teverovsky, "Thermal Shock Testing and Fracturing of MLCCs under Manual Soldering Conditions," *IEEE Transactions on Device and Materials Reliability* vol. 12, pp. 413-419, 2012.

[16] P. C. Dow, "An Analysis of Certain Errors in Electronic Differential Analyzers II-Capacitor Dielectric Absorption," *Electronic Computers, IRE Transactions on,* vol. EC-7, pp. 17-22, 1958.

[17] M. Dawber, K. M. Rabe, and J. F. Scott, "Physics of thin-film ferroelectric oxides," *Reviews of Modern Physics,* vol. 77, pp. 1083-1130, Oct 2005.

[18] J. G. Simmons, "Richardson-Schottky effect in solids," *Physical Review Letters,* vol. 15, pp. 967-968, 1965.